Original Research Article

Influence of telomerase activity and initial distribution on human follicular aging: Moving from a discrete to a continuum model

A.M. Portillo [a,b,*], E. Varela [c,e], J.A. García-Velasco [c,d,e]

[a] Instituto de Investigación en Matemáticas de la Universidad de Valladolid, Valladolid, Spain
[b] Departamento de Matemática Aplicada, Escuela de Ingenierías Industriales, Universidad de Valladolid, Pso. Prado de la Magdalena 3–5, Valladolid, 47011, Spain
[c] IVI Foundation, The Health Research Institute La Fe (IIS La Fe), Edificio Biopolo. Av. Fernando Abril Martorell, 106 – Torre A, Planta 1, Valencia, 46026, Spain
[d] IVIRMA Madrid, Av. del Talgo, 68, Madrid, 28023, Spain
[e] Rey Juan Carlos University, Edificio Departamental II. Av. de Atenas, s/n, Alcorcón, Madrid, 28922, Spain

ARTICLE INFO

ABSTRACT

A discrete model is proposed for the temporal evolution of a population of cells sorted according to their telomeric length. This model assumes that, during cell division, the distribution of the genetic material to daughter cells is asymmetric, i.e. chromosomes of one daughter cell have the same telomere length as the mother, while in the other daughter cell telomeres are shorter. Telomerase activity and cell death are also taken into account. The continuous model is derived from the discrete model by introducing the generational age as a continuous variable in $[0, h]$, being h the Hayflick limit, i.e. the number of times that a cell can divide before reaching the senescent state. A partial differential equation with boundary conditions is obtained. The solution to this equation depends on the initial telomere length distribution. The initial and boundary value problem is solved exactly when the initial distribution is of exponential type. For other types of initial distributions, a numerical solution is proposed. The model is applied to the human follicular growth from preantral to preovulatory follicle as a case study and the aging rate is studied as a function of telomerase activity, the initial distribution and the Hayflick limit. Young, middle and old cell-aged initial normal distributions are considered. In all cases, when telomerase activity decreases, the population ages and the smaller the h value, the higher the aging rate becomes. However, the influence of these two parameters is different depending on the initial distribution. In conclusion, the worst-case scenario corresponds to an aged initial telomere distribution.

1. Introduction

Telomeres are nucleoprotein structures located at distal ends of linear chromosomes. In vertebrates they consist of repetitions of the $5' - TTAGGG - 3'$, repeated up to approximately 10–15 kbp in humans [1–4]. Telomeric DNA is coated by a protein complex called Shelterin, which protect telomeres from fusions, degradation and from being recognized as DNA-damage sites [5]. Telomeres shorten during cell division because the replication machinery cannot copy the very ends of chromosomes (called the end-replication problem) [6] ultimately impairing cell cycle division and leading to cell senescence or apoptosis [3,7]. In humans, telomere loss is approximately of 70 bp per year [8]. Telomerase is an enzyme that can add de novo repeats onto telomeres [9,10] thus, maintaining proper telomere structure. However, telomerase is inactive in most cells of the organism and remains active only in embryonic and adult stem cells, in cancer cells and the germline [3].

Indeed, granulosa cells (GCs), cumulus cells have active telomerase, despite of being somatic cells, and the oocyte also has active telomerase, which is important to preserve genome integrity during meiosis and avoid aneuploidies in the embryo development [4,11,12]. One or several layers of Granulosa cells surround the oocyte to form structures called follicles [13]. At menarche ovaries will have about 300,000 to 400,000 primordial follicles (oocyte arrested in meiosis and one layer of GCs), ready for activation and maturation [14]. Upon activation, oocytes resume meiosis and GCs enter cell division [15], and undergo intense mitotic activity to form antral follicles ready to ovulation. The telomerase activity present in GCs, will possibly facilitate cell division [4], by maintaining telomere length [16] and avoiding chromosome errors that may lead to aneuploidies [4].

There are several mathematical models dealing with telomere shortening: deterministic models with constant telomere loss [17,18] or telomere loss dependent on telomere length [19], as well as stochastic models [20]. In particular, Wattis and colleagues conducted a very interesting study [21] which uses partial differential equations to describe how the distribution of telomere lengths evolves. However, neither

telomerase activity nor cell death are considered in these continuum models.

In an earlier article [22], a dynamical mathematical model was proposed, in which cells were sorted according to their telomeric length. The model was based on the work presented in [23], by using a simple chemical master equation formalism. Telomerase activity and cell death were included in the mathematical modeling and a symmetrical distribution of chromosomes during cell division was assumed, i.e. when a cell divides, it produces two daughter cells with shorter telomeres, due to the end-replication problem and mild oxidation. In [24] we modified the previous model to include higher level of oxidation to accelerate telomere shortening [25]. In this work, first we consider a discrete model taking on asymmetrical distribution of the genomic material into the daughter cells, i.e. one daughter cell has the same telomere length as the mother cell, while the other one has shorter telomeres. Then, we derived the continuum counterpart model where the generational age associated to the telomere length is a continuous variable which varies between zero and the Hayflick limit, where cells cannot divide any longer because they are senescent.

2. Mathematical models

2.1. Discrete mathematical modeling: telomere shortening due to the end replication problem

The generational age of a cell was associated with its telomere length, no matter when it was formed, as in [23]. Telomere length was assessed on the cell level by considering the average telomere length of the cell. We assumed the average telomere length of a cell shortens by a constant factor during each division. The Hayflick limit is the point at which telomeric length is minimal and does not allow replication. Let h denote the proliferation potential, then we considered a finite number of $h + 1$ telomere states of cells, where each state i contains cells of equal average telomere length and the generational age of a cell subpopulation was indicated by subscript i, for $i = 0, 1, \ldots, h-1, h$. Then, cells with maximum telomeric length were considered as generational age of zero and were denoted by C_0, cells whose telomeric length was strictly between the maximum and the minimum value $C_1, \ldots, C_{h-1}$, which can replicate, and senescent cells C_h, which have reached the Hayflick limit.

Let $N_i(t)$, for $i = 0, 1, \ldots, h - 1, h$, denote the population of cells of each generational age at a given time t. Let m be the rate of mitotic replication per cell per unit of time. When $i \neq h$, a cell can undergo mitosis to produce two cells, one of them of the same generational age as the mother and another one a generation older, unlike the former model [22], where symmetrical replication was considered and both daughter cells were assumed to have shorter telomeres. Let d be the rate of mortality events per cell per unit of time. Cells of any generation are susceptible to death. Let r be the rate of telomerase activity per cell per unit of time which acts rejuvenating the cell by lengthening telomeres and moving back to the previous generational age. Only $i \neq 0$ cells are susceptible of rejuvenation by telomerase.

If all rates are taken constant, the average subpopulations $N_0, N_1, \ldots, N_h$ satisfy the following coupled linear ordinary differential equations

$$N_0'(t) = -dN_0(t) + rN_1(t), \tag{1}$$

$$N_i'(t) = mN_{i-1} - (d + r)N_i(t) + rN_{i+1}(t), \ i = 1, \ldots, h - 1, \tag{2}$$

$$N_h'(t) = mN_{h-1} - (d + r)N_h(t). \tag{3}$$

Denoting by $\mathbf{N}(t) = [N_0, N_1, \ldots, N_h]^T$ the system of Eqs. (1)–(3) can be rewritten as

$$\mathbf{N}'(t) = A\mathbf{N}(t), \tag{4}$$

where

$$A = \begin{pmatrix} -d & r & 0 & \cdots & & 0 \\ m & -(d+r) & r & 0 & & 0 \\ \vdots & \ddots & \ddots & \ddots & & \vdots \\ 0 & \cdots & m & -(d+r) & & r \\ 0 & \cdots & & 0 & m & -(d+r) \end{pmatrix} \tag{5}$$

is a tridiagonal matrix of dimension $(h + 1) \times (h + 1)$.

The solution of the system with matrix (5) preserves positivity, i.e. a nonnegative initial condition leads to a nonnegative solution over time. The proof is similar to the one in [24].

2.2. Continuum counterpart model to classify a population according to the generational age

In this subsection, a partial differential equation and boundary conditions from the discrete model is derived. Let x be the continuous variable representing the generational age $x \in [0, h]$ and $N(x, t)$ the population density at generational age x and time t. The following initial and boundary value problem (IBVP) is considered as the continuum counterpart model

$$N_t(x, t) = \frac{1}{2}(m + r)N_{xx}(x, t) - (m - r)N_x(x, t)$$

$$+ (m - d)N(x, t), \ 0 < x < h, t > 0, \tag{6}$$

$$\frac{1}{2}(m + r)N_x(0, t) - (m - r)N(0, t) = 0, \ t > 0, \tag{7}$$

$$\frac{1}{2}(m + r)N_x(h, t) - (m - r)N(h, t) = 0, \ t > 0, \tag{8}$$

$$N(x, 0) = f(x), \ 0 < x < h. \tag{9}$$

The Eq. (6) is a diffusion–advection equation which presents a description of the growth of the population. The term $\frac{1}{2}(m + r)N_{xx}$ represents the random diffusion of the population with a diffusive coefficient $\frac{1}{2}(m + r)$. The term $-(m - r)N_x$ renders the advective flow with an advective coefficient $m - r$. The growth rate of the population is $m - d$. The Eqs. (7) and (8) give the boundary conditions and the last equation represents the initial distribution of the population which must be regular enough and compatible with the boundary conditions.

A justification of how we have arrived at this initial and boundary value problem is given below. From the discrete model (1)–(3) in which the generational age takes integer values, now it is considered the generational age as a continuous variable x and $N(x, t)$ the population density at generational age x and time t

$$N_t(x, t) = mN(x - 1, t) - (d + r)N(x, t) + rN(x + 1, t), \ 0 < x < h, t > 0. \tag{10}$$

Approximating $N(x - 1, t)$ and $N(x + 1, t)$ by their 2nd-degree Taylor polynomial in the variable x we achieve the following equation

$$N_t(x, t) = (m - d)N(x, t) + (r - m)N_x(x, t)$$

$$+ \frac{m + r}{2}N_{xx}(x, t), \ 0 < x < h, t > 0. \tag{11}$$

We assign Robin type boundary conditions that make sense from a biological point of view. The Robin type boundary conditions have to guarantee that no cell population density $N(x, t)$ either leaves or enters the interval $x \in [0, h]$, that is, they have to ensure zero-flux requirement at $x = 0$ and at $x = h$. Conditions (7) and (8) have been derived from (6) so that there is no zero-flux at the boundary.

For any nonnegative initial conditions, by the maximum principle [26] and the standard theory for parabolic equations [27], the IBVP (6)–(9) admits a unique positive smooth solution which exists globally in time.

2.2.1. Qualitative study

Theorem 1. *Assuming that $0 < r < m$ in the IBVP (6)–(9) and the initial density is compatible with the boundary conditions and C^2 continuous, then the population density at generational age x and time t can be expressed in terms of the parameters of the model as*

$$N(x,t) = \exp(\lambda t)\exp(\mu x)\sum_{n=0}^{\infty} a_n \varphi_n(x)\exp\left(-\frac{(m+r)\lambda_n}{2}t\right), \quad (12)$$

where

$$\lambda = m - d - \frac{(m-r)^2}{2(m+r)}, \quad \mu = \frac{m-r}{m+r}, \quad (13)$$

the eigenvalues and related eigenfunctions

$$\lambda_0 = -\mu^2, \quad \varphi_0 = \exp(\mu x), \quad (14)$$

$$\lambda_n = \left(\frac{n\pi}{h}\right)^2, \quad \varphi_n = \cos\left(\frac{n\pi x}{h}\right) + \frac{\mu h}{n\pi}\sin\left(\frac{n\pi x}{h}\right), \quad n = 1, 2, \ldots, \quad (15)$$

and

$$a_n = \frac{\int_0^h f(\xi)\exp(-\mu\xi)\varphi_n(\xi)d\xi}{\int_0^h \varphi_n^2(\xi)d\xi}, \quad n = 0, 1, 2, \ldots. \quad (16)$$

Proof. Let us define the quantities

$$D = \frac{m+r}{2}, \quad v = m - r, \quad \rho = m - d. \quad (17)$$

Since the diffusion–advection partial differential equation (6) is linear, homogeneous, and has constant coefficients, then, by using the following transformation,

$$N(x,t) = S(x,t)\exp\left[\left(\rho - \frac{v^2}{4D}\right)t + \frac{vx}{2D}\right], \quad (18)$$

the partial differential equation (6) reduces to a standard diffusion equation. The IBVP for the auxiliary function $S(x,t)$ reads as

$$S_t(x,t) = DS_{xx}(x,t), \quad 0 < x < h, t > 0, \quad (19)$$

$$S_x(0,t) - \frac{v}{2D}S(0,t) = 0, \quad t > 0, \quad (20)$$

$$S_x(h,t) - \frac{v}{2D}S(h,t) = 0, \quad t > 0, \quad (21)$$

$$S(x,0) = f(x)\exp\left(-\frac{vx}{2D}\right), \quad 0 < x < h. \quad (22)$$

Notice that

$$\rho - \frac{v^2}{4D} = \lambda, \quad \frac{v}{2D} = \mu. \quad (23)$$

To solve the IBVP (19)–(22), we only require to consider the separated solution $S(x,t) = \varphi(x)T(t)$. This leads to a regular Sturm–Liouville problem, which is solved in [28], with the eigenvalues and related eigenfunctions

$$\lambda_0 = -\mu^2, \quad \varphi_0 = \exp(\mu x),$$

$$\lambda_n = \left(\frac{n\pi}{h}\right)^2, \quad \varphi_n = \cos\left(\frac{n\pi x}{h}\right) + \frac{\mu h}{n\pi}\sin\left(\frac{n\pi x}{h}\right), \quad n = 1, 2, \ldots,$$

Then the expression (12) is obtained.

The qualitative study is important because it gives an idea of the influence of the model parameters on the solution. Although the expression is valid for many initial conditions, the difficulty lies in the calculation of the coefficients a_n. For example, for an initial density function of Gaussian type, the primitives of the integrals cannot be obtained as a finite sum of elementary functions and in practice the problem has to be solved numerically.

2.2.2. Aging rate

The average number of cells of generational age less than or equal to x at a given time t is denoted by

$$n(x,t) = \int_0^x N(\omega,t)d\omega. \quad (24)$$

Fixed a number q, we considered the population of aged cells at a given time t, the average number of cells of generational age between $h - q$ and h

$$a(t) = \int_{h-q}^h N(\omega,t)d\omega. \quad (25)$$

We defined the aging rate a_r as the number of aged cells divided by the total number of cells, that is

$$a_r(t) = \frac{a(t)}{n(h,t)} = 1 - \frac{n(h-q,t)}{n(h,t)}. \quad (26)$$

The values of a_r may vary between 0 and 1. Values of a_r close to 0 corresponded to populations of young cells, while the closer to 1 the value was, the older the population was.

If the initial condition in (9) is

$$f(x) = \exp(2\mu x), \quad (27)$$

then

$$N(x,t) = \exp(\lambda t)\exp(2\mu x)\exp\left(-\frac{(m+r)\lambda_0}{2}t\right), \quad (28)$$

$$n(x,t) = \exp(\lambda t)\exp\left(-\frac{(m+r)\lambda_0}{2}t\right)\frac{\exp(2\mu x) - 1}{2\mu}, \quad (29)$$

and the corresponding aging rate is

$$a_r(t) = 1 - \frac{\exp(2\mu(h-q)) - 1}{\exp(2\mu h) - 1}. \quad (30)$$

Remark 1. If the initial distribution is (27), as in Theorem 1, the aging rate depends on h and on μ, which in turn depends on the relation between the parameters m and r. We introduce the parameter s, $0 < s < 1$, such that $r = sm$, in order to rewrite μ in terms of this single parameter

$$\mu = \frac{1-s}{1+s} \quad (31)$$

and thus study the influence of the amount of telomerase activity on aging. Values of s close to 0 represent low telomerase activity, while values of s close to 1 indicate high telomerase activity.

Fig. 1 displays the influence of h and s on the aging rate, considering $0.7 < s < 1$, for $h = 40, 50, 60$. Taking $h = 50$ as a reference, we assume as aged cells those in the last third of the interval and therefore we choose $q = 51/3 = 17$. For a value of s less than 0.8 the aging rate is close to 1 in all cases, regardless of h. As s approaches 1, that is, when r is near m, the aging rate decreases with a steeper slope the higher h.

3. Human follicular growth from preantral to preovulatory follicle as a case study

We focused the study on the evolution of the population of GCs which are the most important somatic cells for determining the size of follicles [29]. Human preantral follicles take approximately 85 days to reach preovulatory size, according to Gougeon classification [30], going through eight classes, from class 1 for preantral follicle to class 8 for preovulatory follicle. Fig. 2 displays a scheme of the classification of follicles in the human ovary according to Gougeon [30], where the transition time of each stage and the total number of GCs in each stage are shown.

We assumed the population of GCs in each of the eight stages corresponding to the development of the follicle from preantral to preovulatory class satisfied a initial–boundary value problem similar to the one of Section 2.2, with partial differential equation

$$N_t(x,t) = \frac{1}{2}(m_j + r_j)N_{xx}(x,t) - (m_j - r_j)N_x(x,t)$$
$$+ (m_j - d_j)N(x,t), 0 < x < h, t \in [T_j, T_{j+1}], \quad (32)$$

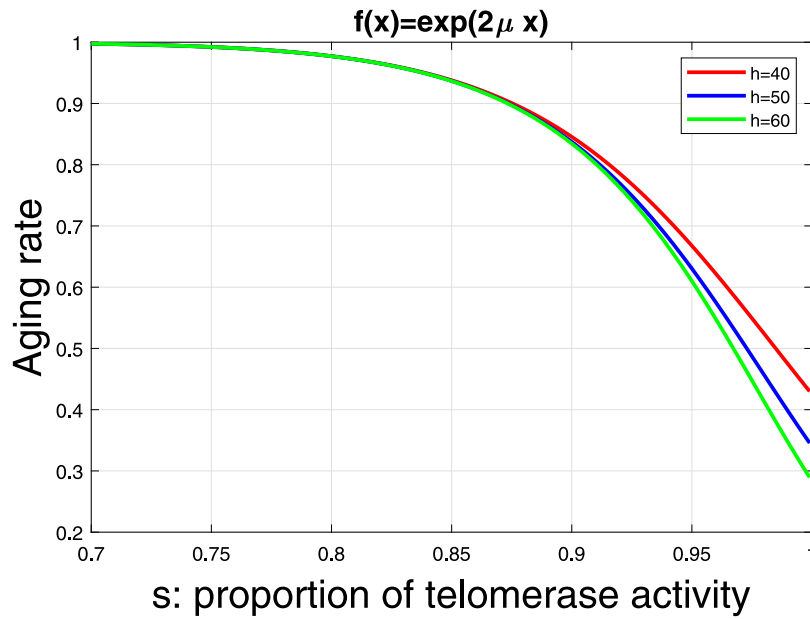in which the values m_j, d_j and r_j correspond to the class j from 1 to 7.

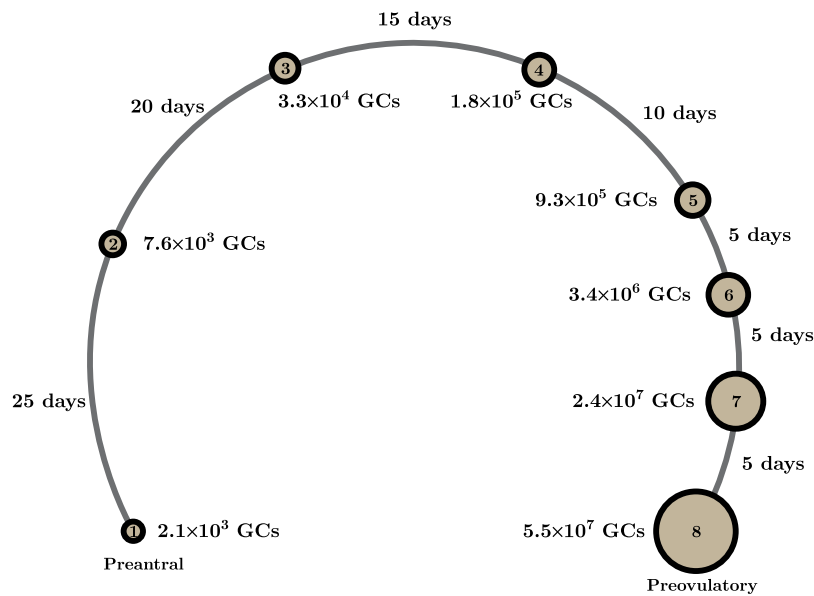**Fig. 1.** Aging rate versus s, for $h = 40, 50, 60$.

Fig. 2. Classification from preantral to preovulatory follicles in the human ovary based on data from [30].

In order to calculate the model parameters, the values of the times T_j and the total number of GCs at T_j, $\tilde{n}_j$, have been taken from [30] data. Considering the discrete model in Section 2.1, the total number of cells $n_j(t)$ in the transit time from stage j to $j+1$ approximately meets

$$n_j'(t) = (m_j - d_j)n_j(t),\ t \in [T_j, T_{j+1}], \tag{33}$$

$$n_j(T_j) = \tilde{n}_j, \tag{34}$$

from which is obtained the expression

$$n_j(T_{j+1}) = \tilde{n}_j \exp((m_j - d_j)(T_{j+1} - T_j)) = \tilde{n}_{j+1}, \tag{35}$$

and then the difference between the mitosis rate and the mortality rate for each follicle class was estimated as

$$m_j - d_j = \log(\tilde{n}_{j+1}/\tilde{n}_j)/(T_{j+1} - T_j) = \beta_j,\ \text{for } j = 1, \ldots, 7. \tag{36}$$

4. Numerical experiments

In former work [24], different percentiles of telomere length of GCs according to chronological age were studied, as can be seen in Table 2, where values of division capacity for GCs for different percentiles at 25 and 40 years old are shown. Thus, $h = 40$ occurs in the average of women in their forties and in younger women in lower percentiles, whose biological age is older than their chronological age. Meanwhile $h = 50$ is a value near the average among women aged 25 years and $h = 60$ corresponds to higher percentiles, meaning the biological age is younger than the chronological age. Taking this into account, in the numerical experiments, we consider the values of $h = 40, 50, 60$ to cover several percentiles at the ages of 25 and 40.

Mortality rates were fixed at 0.01 day^{-1} in the numerical experiments. The computed values $m_j = \beta_j + d_j$ and telomerase activity rates
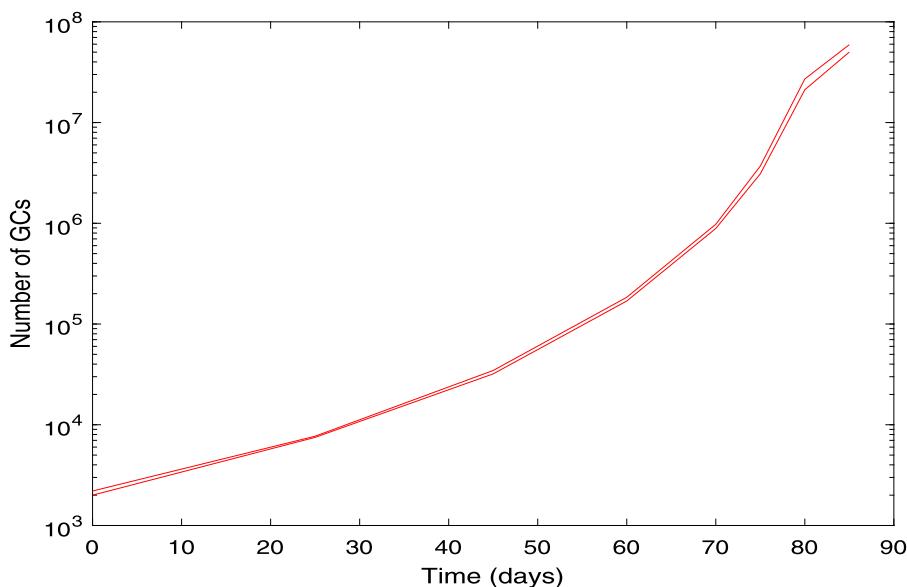
Fig. 3. Maximum and minimum number of GCs that can exist from preantral to preovulatory follicle, according to Gougeon [30].

Table 1
Mitosis and telomerase activity rates for each follicle class. The values m_j were computed as $\beta_j + 0.01$, using the values of β_j in (36) with Gougeon [30] data.

Follicle class	1	2	3	4	5	6	7
m_j	0.0614	0.0839	0.1213	0.1764	0.2685	0.4020	0.1738
$r_j = 0.95 m_j$	0.0584	0.0797	0.1152	0.1676	0.2551	0.3819	0.1651
$r_j = 0.75 m_j$	0.0461	0.0629	0.0910	0.1323	0.2014	0.3015	0.1304
$r_j = 0.55 m_j$	0.0338	0.0461	0.0667	0.0970	0.1477	0.2211	0.0956

Table 2
Aging rates for a initial density function of exponential type with $s = 0.99$.

h	a_r
40	0.43
50	0.35
60	0.30

for different values of the parameter s for each follicle class are showed in Table 1. In the numerical experiments we made sure that the total population of GCs obtained was within the Gougeon limits [30], shown in Fig. 3.

4.1. Initial density function of exponential type

To check that the numerical results correspond to the theoretical results, we considered an initial density function such as the one in (27)

$$N(x, 0) = C \exp(2\mu x), \tag{37}$$

for

$$s = 0.99, \quad \mu = \frac{1-s}{1+s}, \tag{38}$$

$$C = \frac{4200\mu}{(e^{2\mu h} - 1)}. \tag{39}$$

The aging rates obtained with the discrete model for the values of $h = 40, 50$ and 60, for the final time 85 are shown in Table 2. It can be seen that they coincide with those shown in Fig. 1.

4.2. Initial density function of Gaussian (normal) type

Next we studied another type of initial conditions, namely the normal density functions, for which the expression of the exact solution

of the continuous model cannot be found, but its numerical solution can be obtained.

$$N(x, 0) = \frac{2100}{\sqrt{2\pi\sigma^2}} e^{-(x-\nu)^2/2\sigma^2}. \tag{40}$$

The initial conditions are heterogeneous depending on the individual, but we have tried to reproduce several biologically plausible scenarios to help us see the trend of the population's evolution. In the following experiments σ was fixed to 4 and three values of ν were taken, which were $h/4$, with the initial density function centered on the first quarter of the interval, $h/2$, with the initial density function centered at the midpoint of the interval, and $3h/4$, with the initial density function centered on the third quarter of the interval. In all cases the total population of GCs obtained was within the limits set by in [30]. Fig. 4 showed just one example, for $h = 50$, $s = 0.5$ and $\nu = h/2$, the limits estimated in [30] for the total population of GCs for the different stages from preantral to preovulatory follicle in red, and in blue the values obtained by the model.

4.2.1. Q1 initial distribution: $\nu = h/4$

Fig. 5 displays the evolution of the density function at day 0 (left graphs) and after 85 days (right graphs) when the initial distribution is a Gaussian distribution centered on the first quarter of the interval $[0, h]$, over which telomere lengths vary, for h equal to 40 (Fig. 5(a) and (b)), 50 (Fig. 5(c) and (d)) and 60 (Fig. 5(e) and (f)). The distribution at day 85 is shown for five values of the parameter s, which relates telomerase activity to the mitosis ratio, i.e. $r_j = sm_j$, for the seven stages of follicular development considered. Regardless of the value of h, the shape of the distribution remains the same but as s decreases (i.e. telomerase activity decreases), the distribution shifts to the right and the maximum increases, meaning that the mean increases and the variance decreases. As a consequence, when telomerase activity decreases, the population ages. The influence of the value of h and the parameter s on the aging rate at day 85 is displayed in Fig. 5(g). The aging rate decreases as the parameter s increases, meaning that as the telomerase activity increases, the telomere maintenance in cells would prevent aging. The smaller the h is the higher the aging rate becomes. Although it must be said that for this initial condition the aging rate is always small, especially for $h = 50, 60$.
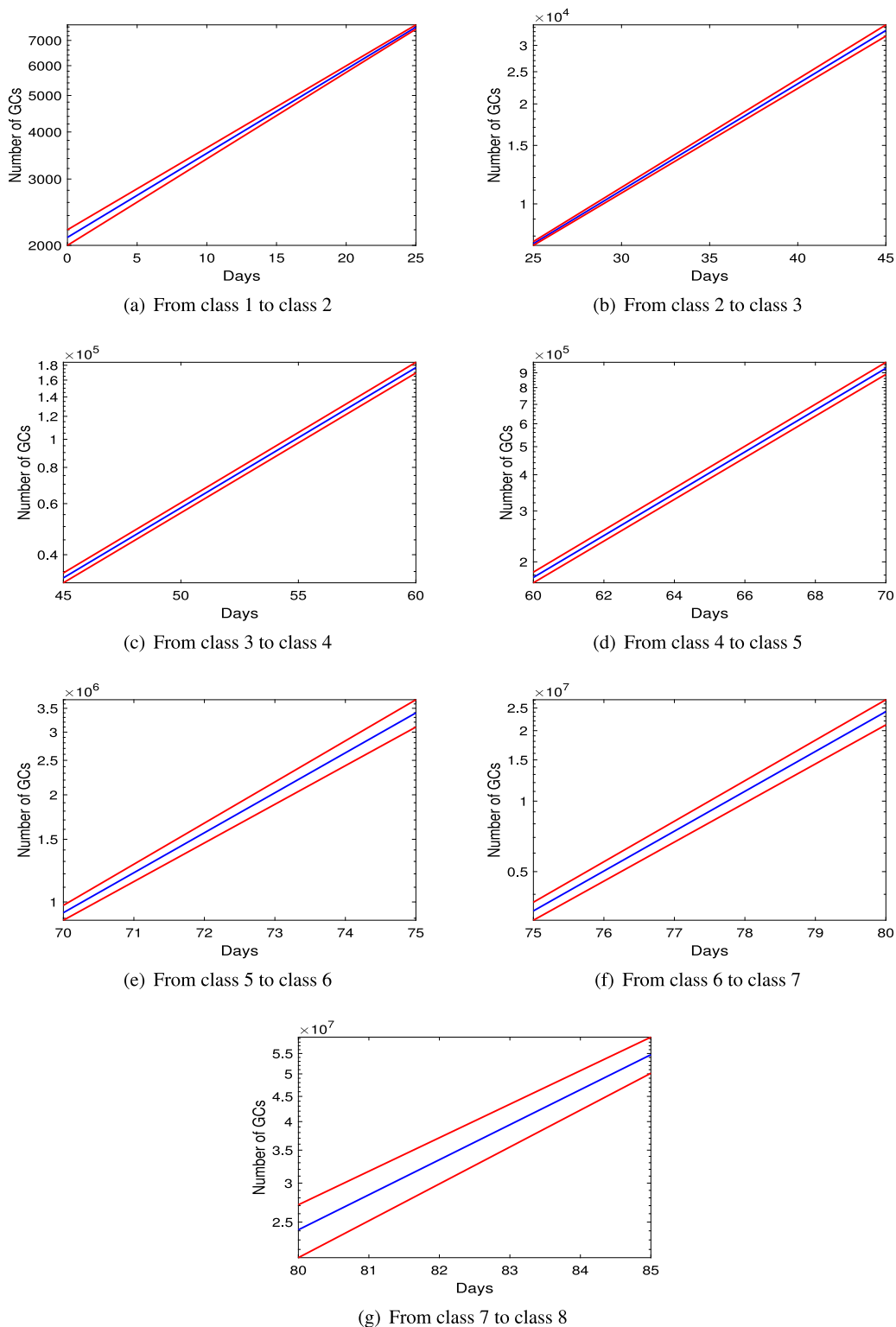
Fig. 4. Total population of GCs from preantral to preovulatory follicle: limits estimated in [30] in red and values obtained by the model in blue, for $h = 50$, $s = 0.5$ and Gaussian initial density with $v = h/2$.

4.2.2. Q2 initial distribution: $v = h/2$

Fig. 6 displays the evolution of the density function at day 0 (left graphs) and after 85 days (right graphs) when the initial distribution is a Gaussian distribution centered on the first quarter of the interval $[0, h]$, for h equal to 40 (Fig. 6(a) and (b)), 50 (Fig. 6(c) and (d)) and 60 (Fig. 6(e) and (f)). As in the previous case, the final distribution is

shown for five values of the parameter s, and can also be observed that as s decreases the distribution shifts to the right, i.e. to more aged zone, indicating that when telomerase activity decreases, the population ages. The influence of the value of h and the parameter s on the aging rate at day 85 is displayed in Fig. 6(g). Similar comments can be made as in the previous case. However, for this initial condition, the value of h
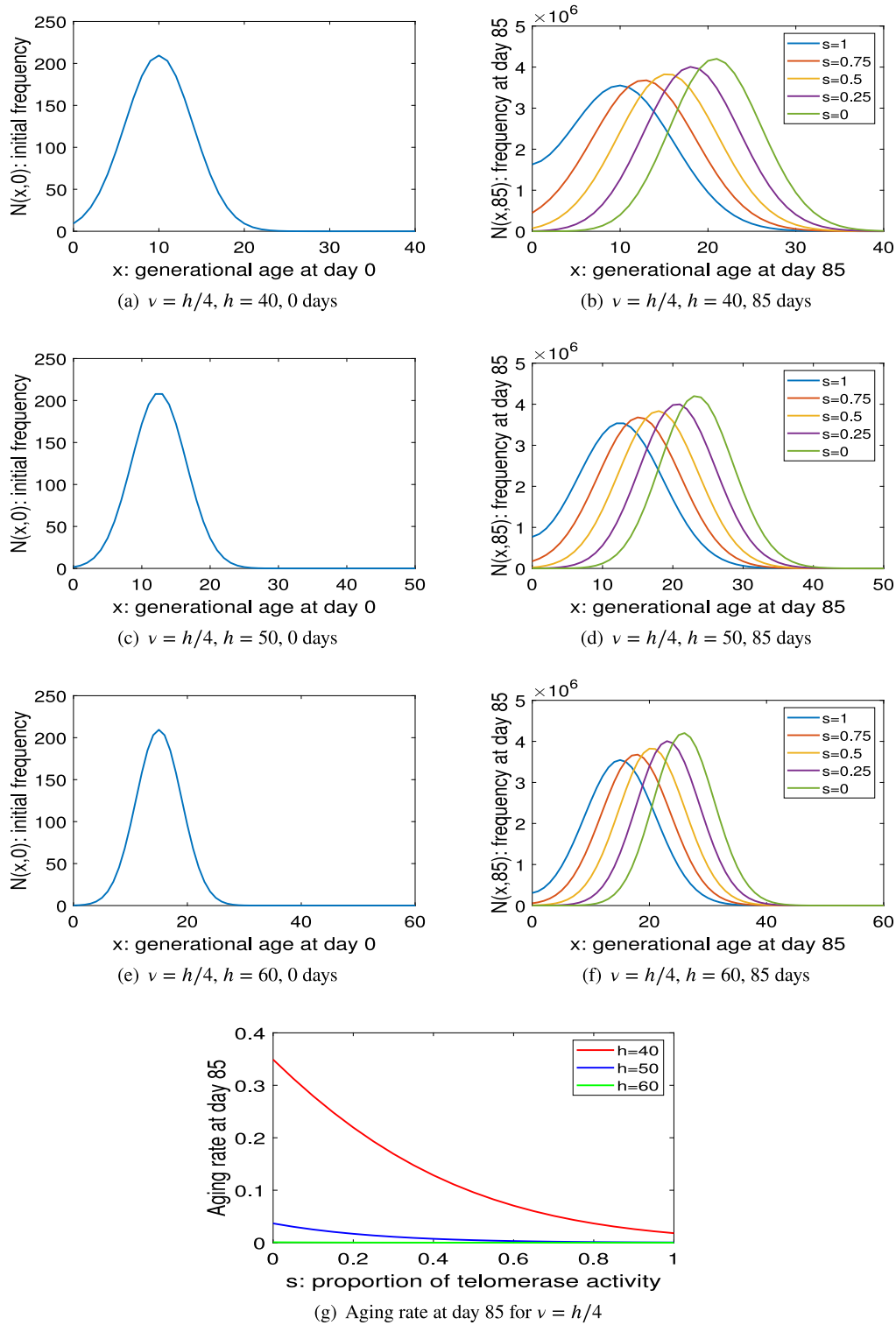
(a) $v = h/4$, $h = 40$, 0 days

(b) $v = h/4$, $h = 40$, 85 days

(c) $v = h/4$, $h = 50$, 0 days

(d) $v = h/4$, $h = 50$, 85 days

(e) $v = h/4$, $h = 60$, 0 days

(f) $v = h/4$, $h = 60$, 85 days

(g) Aging rate at day 85 for $v = h/4$

Fig. 5. Evolution of the density function for a young Q1 initial distribution of Gaussian type.

is more important than in the previous case. Let us look, for example, at the values for $s = 0$, for which the differences between the values of h are substantial: for $h = 40$ the aging rate is above 0.9, for $h = 50$ above 0.7 and for $h = 60$ above 0.3. For lower values of h the amount of telomerase activity is substantial to decrease the aging rate.

4.2.3. Q3 initial distribution: $v = 3h/4$

Fig. 7 displays the evolution of the density function at day 0 (left graphs) and after 85 days (right graphs) when the initial distribution

is a Gaussian distribution centered on the first quarter of the interval $[0, h]$, for h equal to 40 (Fig. 7(a) and (b)), 50 (Fig. 7(c) and (d)) and 60 (Fig. 7(e) and (f)).

In the same way as for the previous two initial conditions, the final distribution is shown for five values of the parameter s, and it is also noted that as s decreases the distribution shifts to the right, with a concentration of the population in the older part of the range. Fig. 7(g) exhibits the influence of s and h on the aging rate on day 85. The smaller s and h the higher the aging rate. This time, nevertheless, the

(a) $v = h/2$, $h = 40$, 0 days

(b) $v = h/2$, $h = 40$, 85 days

(c) $v = h/2$, $h = 50$, 0 days

(d) $v = h/2$, $h = 50$, 85 days

(e) $v = h/2$, $h = 60$, 0 days

(f) $v = h/2$, $h = 60$, 85 days
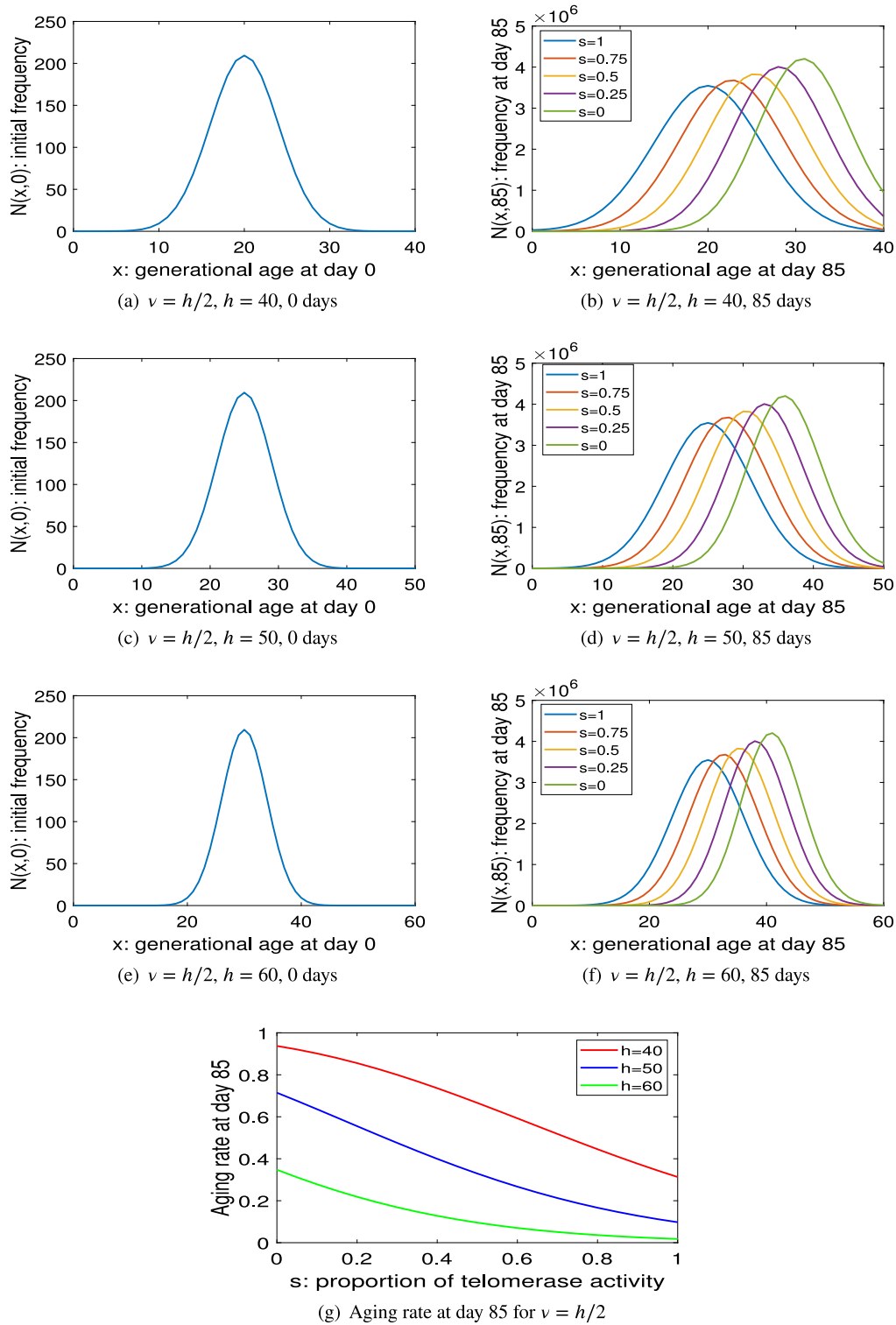
(g) Aging rate at day 85 for $v = h/2$

Fig. 6. Evolution of the density function for a median age Q2 initial distribution of Gaussian type.

situation is far worse. When $s = 0$, independent of h, the aging rate is practically 1. If we now look at the best possible case which is $s = 1$, the aging rates for $h = 40$, 50, 60 are above 0.85, 0.75 and 0.6 respectively, which are quite high values. In conclusion, the worst-case scenario is an aged initial distribution, which leaves little room for the influence of telomerase activity.

To better understand the effect of the initial distribution on the aging rate, we have shown in Fig. 8 the aging rate at day 85, for $h = 40, 50, 60$, versus the mean of the initial distribution. The value

$s = 0$, in red (the upper line), corresponds to no telomerase activity and $s = 1$, in blue (the lower line), to maximum telomerase activity. The results for intermediate telomerase activity values would be between the red and blue curves. For $h = 40$, if the mean initial density is less than 12, the aging rate is less than 0.5 whereas if the initial density is greater than 23, the aging rate is greater than 0.5, independently of telomerase activity. For values of the mean initial density between 12 and 23 there is considerable variation of the aging rate depending on the telomerase activity. For $h = 50$, if the mean initial density
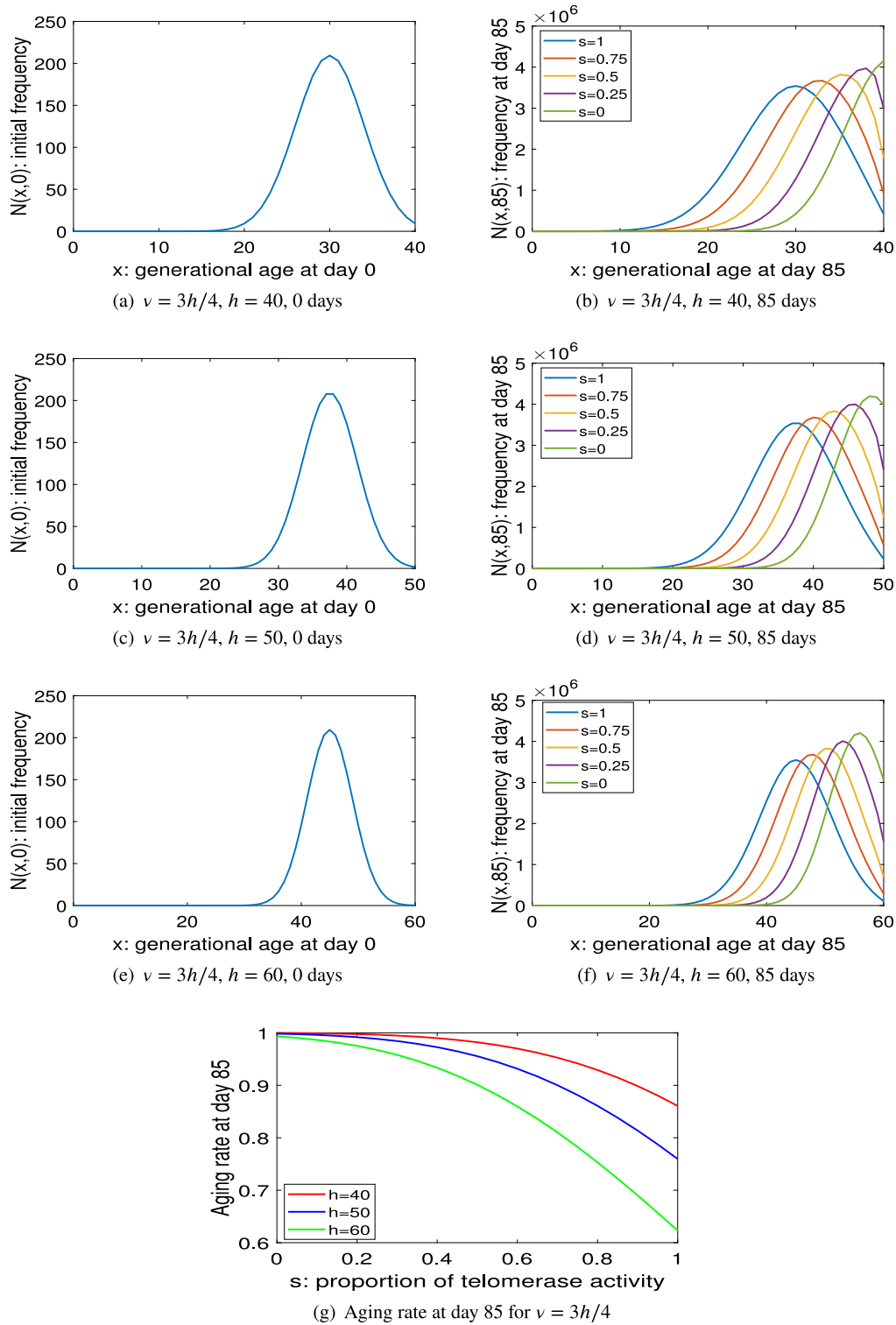
(a) $v = 3h/4$, $h = 40$, 0 days

(b) $v = 3h/4$, $h = 40$, 85 days

(c) $v = 3h/4$, $h = 50$, 0 days

(d) $v = 3h/4$, $h = 50$, 85 days

(e) $v = 3h/4$, $h = 60$, 0 days

(f) $v = 3h/4$, $h = 60$, 85 days

(g) Aging rate at day 85 for $v = 3h/4$

Fig. 7. Evolution of the density function for an aged Q3 initial distribution of Gaussian type.

is less than 22, the aging rate is less than 0.5 whereas if the initial density is greater than 33, the aging rate is greater than 0.5, regardless of telomerase activity. For values of the mean initial density between 22 and 33 there is significant difference of the aging rate according to the telomerase activity. For $h = 40$, if the mean initial density is less than 32, the aging rate is less than 0.5 whereas if the initial density is greater than 43, the aging rate is greater than 0.5, irrespective of telomerase activity. For values of the mean initial density between 32

and 43 there is substantial change of the aging rate in terms of the telomerase activity.

5. Discussion

Here we have examined the degree of cell aging during follicular development on the bases of the aging state of the initial population of cells, according to the number of divisions that cells can undergo before
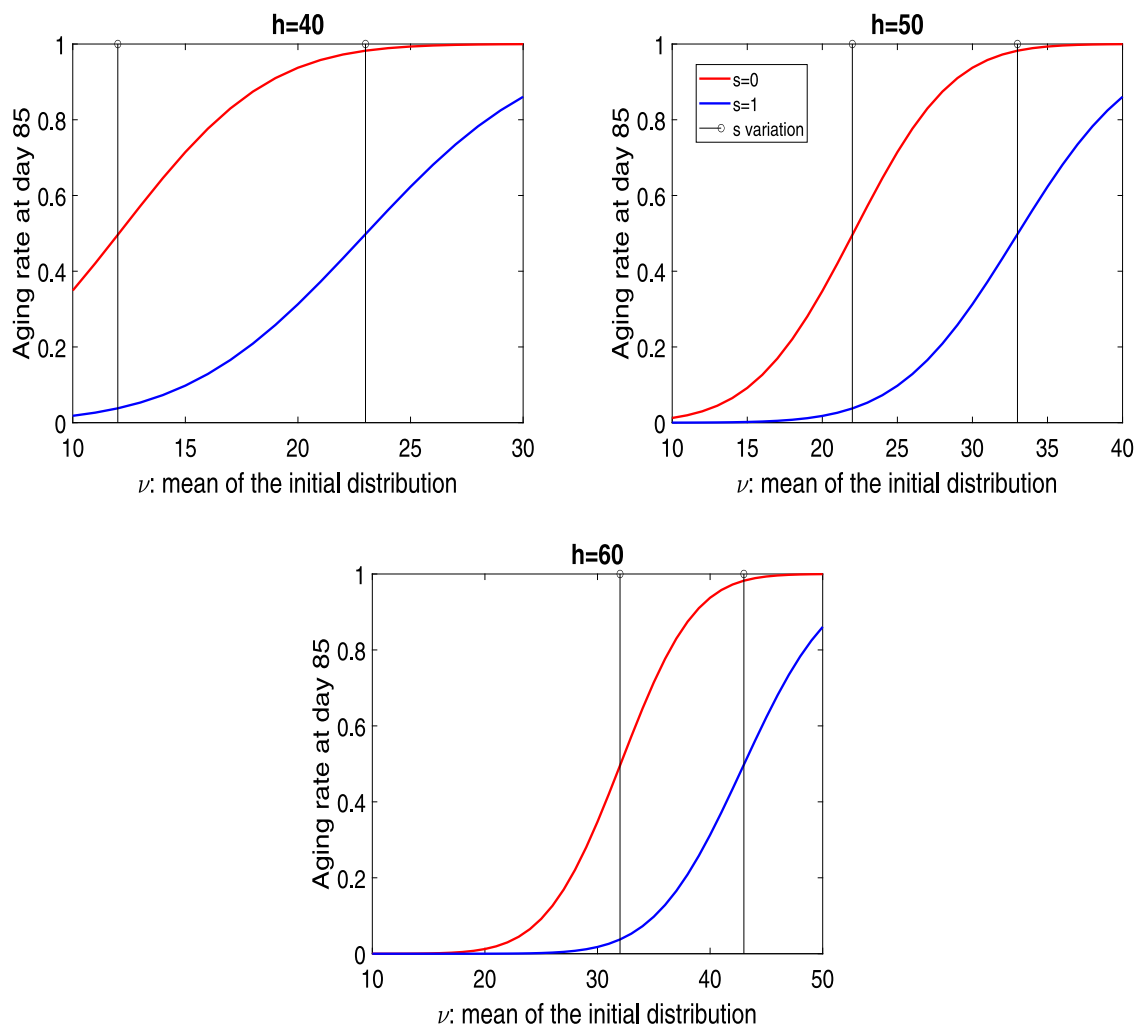
Fig. 8. Aging rate at day 85, for $h = 40, 50, 60$, versus the mean of the initial distribution. The value $s = 0$, in red, corresponds to no telomerase activity and $s = 1$, in blue, to maximum telomerase activity. The outcomes for intermediate telomerase activity values would be between the red and blue curves.

reaching the point of reproductive senescence and the proportion of telomerase activity. To this end, a discrete mathematical model which assumes asymmetrical distribution of the genetic material has been proposed. A continuum model has been derived from the discrete model by introducing the generational age as a continuous variable. The solution to the partial differential equation is found when the initial distribution of ages is exponential, whereas, for other types of initial distribution, a numerical solution is proposed.

In biological studies there are several distributions that are commonly used. One of them is the exponential distribution, which takes into account the age heterogeneity of the population. For this initial distribution case, the solution of the equation was exact, however, a limitation for the value of the s parameter was found. For s values lower than 0.95 the number of cells did not properly fit the limits described by Gougeon [30]. To solve this point, a normal distribution was used, which is also commonly applied to biological problems. The analysis by Wattis et al. [21] indicated that constant telomere loss leads to a Gaussian (normal) distribution of telomere lengths. In this case, the number of cells obtained were always within the limits described by Gougeon [30]. Thus, this type of distribution seemed more appropriate for the analysis of cell aging during folliculogenesis.

To analyze the evolution of cell aging in young individuals (10 to 25 years old), which still have an overage telomere length of around 8 to 12 kb [31], the initial distribution was located in the first quartile, where the number of cell divisions was still high before reaching cellular senescence, regardless of the h value used. Under this condition, even

those cells with less division potential ($h = 40$), and in the absence of telomerase, were below the middle value of aging rate (0.5), meaning that the whole population of cells at the end of the folliculogenesis process was relatively young. The influence of telomerase activity was more noticeable on cells with the lowest division potential ($h = 40$) compared to younger cells ($h = 50$ or 60). In the presence of high telomerase activity, all cells were juvenile at day 85 of development with aging rates below 0.1. Thus, according to the model, young populations of cells with good levels of telomerase activity would remain juvenile after folliculogenesis. Juvenile cells would be found in healthy younger women, where GCs would have the potential to better support oocyte maturation [14].

With an initial distribution in the second quartile, which would resemble relatively aged cells, with shorter telomere lengths, and therefore, lower division potential for follicular development, the cell population had a higher aging rate at the end of folliculogenesis. Particularly, the cells with less division potential ($h = 40$) and with normal division potential ($h = 50$) were aged in the absence of telomerase, with an aging rate close to 1, at the limit of reproductive senescence. Only cells with high division potential would remain juvenile (aging rate below 0.4). In the presence of high telomerase activity ($s = 0.85$), the aging rate would still not be dramatic at the end of folliculogenesis (values below 0.5). A similar behavior is observed for cells with a better division potential ($h = 50$). Lastly, cells with the highest division potential ($h = 60$) would remain juvenile after follicle development.

These results could resemble middle-age women with premature ovarian failure, which have shorter telomere length in their GCs and low or null telomerase activity [32,33] compared to aged-matched controls, which would have active telomerase.

Finally, to assess the aging rate in an older cell population, the initial distribution was located in the third quartile, where cells have very low division potential. Under this condition, in cells which do not have telomerase activity, all cell populations were aged after follicular development and even those cells with the highest division potential ($h = 60$) in the presence of higher levels of telomerase would reach the end of follicular development aged. In the presence of increasing proportions of telomerase activity, cells with higher division potential ($h = 60$) were less aged, but still with values above 0.5 for aging rate. These results could reflect what happens in aged women, whose cells bear shorter telomeres due to the action of reactive oxygen species or other lifestyle factors [4,11] Additionally, those aged cell with low or null telomerase activity could reflect patients with telomeropathies, such as dyskeratosis congenita. These patients have shorter mean telomere length for their age [34] and have impaired fertility [35].

The analysis of the effect of the initial distribution on aging rate showed that as the h value increases (cells with more division potential), the point at which the population has aged 0.5 for different proportions of telomerase activity moves towards higher values of mean initial distribution. These results suggest that when cells have more potential to divide, there is a margin for the initial distribution to have older cells without causing severe aging of the population of cells (aging rate below 0.5). In addition, as the h value increases, the red line (the upper line in Fig. 8) was lower in the y axis, leaning towards a more juvenile population. Thus, cells with low telomerase activity and initial distributions with mean exceeding half of the interval still have acceptable aging rates.

According to the mathematical model proposed, younger populations of GCs would have larger division potential and would be more sensitive to the action of telomerase, maintaining a better telomere structure. Indeed, an association between telomere length and oocyte and embryo aneuploidy has been found [36]. Thus, according to the mathematical model, strategies to reactivate telomerase in women with fertility problems should be more successful in young or middle-aged women compared to older women.

An option for future research is to consider a net growth rate $m - d$ being generational age dependent or time dependent.

CRediT authorship contribution statement

A.M. Portillo: Mathematical conceptualization, Formal analysis, Funding acquisition, Investigation, Software, Writing – review & editing. **E. Varela:** Biological conceptualization, Funding acquisition, Investigation, Writing – review. **J.A. García-Velasco:** Funding acquisition, Discussion of results, Review.

Declaration of competing interest

The authors declare that they have no known competing financial interests or personal relationships that could have appeared to influence the work reported in this paper.

Acknowledgments

The authors would like to thank the anonymous reviewers for their valuable comments and suggestions.

References

[1] G. Hotchkiss, P.-O. Pehrson, S. Larsson, L. Ahrlund-Richter, S. Britton, Telomere loss in peripheral blood mononuclear cells may be moderately accelerated during highly active antiretroviral therapy (HAART), J. Acquir. Immune Defic. Syndr. (1999) 22 (5) (1999) 445–452.

[2] A. Melk, V. Ramassar, L.M. Helms, R. Moore, D. Rayner, K. Solez, P.F. Halloran, Telomere shortening in kidneys with age, J. Am. Soc. Nephrol. 11 (3) (2000) 444–453.

[3] E. Varela, M. Blasco, 2009 Nobel prize in physiology or medicine: telomeres and telomerase, Oncogene 29 (11) (2010) 1561–1565.

[4] A.M. Polonio, L. Chico-Sordo, I. Córdova-Oriz, M. Medrano, J.A. García-Velasco, E. Varela, Focus: Sex & reproduction: Impact of ovarian aging in reproduction: From telomeres and mice models to ovarian rejuvenation, Yale J. Biol. Med. 93 (4) (2020) 561.

[5] T. de Lange, Shelterin-mediated telomere protection, Annu. Rev. Genet. 52 (2018) 223–247.

[6] A.M. Olovnikov, A theory of marginotomy: the incomplete copying of template margin in enzymic synthesis of polynucleotides and biological significance of the phenomenon, J. Theoret. Biol. 41 (1) (1973) 181–190.

[7] L. Hayflick, A brief history of the mortality and immortality of cultured cells, Keio J. Med. 47 (3) (1998) 174–182.

[8] E. Vera, B. Bernardes de Jesus, M. Foronda, J. Flores, M. Blasco, The rate of increase of short telomeres predicts longevity in mammals, Cell Rep. 2 (2012) 732–737.

[9] C.W. Greider, E.H. Blackburn, Identification of a specific telomere terminal transferase activity in Tetrahymena extracts, Cell 43 (2) (1985) 405–413.

[10] C.W. Greider, E.H. Blackburn, The telomere terminal transferase of Tetrahymena is a ribonucleoprotein enzyme with two kinds of primer specificity, Cell 51 (6) (1987) 887–898.

[11] L. Chico-Sordo, I. Córdova-Oriz, A.M. Polonio, L.S. S-Mellado, M. Medrano, J.A. García-Velasco, E. Varela, Reproductive aging and telomeres: Are women and men equally affected? Mech. Ageing Dev. 198 (2021) 111541.

[12] I. Córdova-Oriz, L. Chico-Sordo, E. Varela, Telomeres, aging and reproduction, Curr. Opin. Obstet. Gynecol. 34 (3) (2022) 151–158.

[13] E. Telfer, R. Anderson, The existence and potential of germline stem cells in the adult mammalian ovary, Climacteric 22 (1) (2019) 22–26.

[14] A.N. Hirshfield, Development of follicles in the mammalian ovary, Int. Rev. Cytol. 124 (1991) 43–101.

[15] A. Kallen, A.J. Polotsky, J. Johnson, Untapped reserves: controlling primordial follicle growth activation, Trends Mol. Med. 24 (3) (2018) 319–331.

[16] D.C. Pedroso, V.P. Santana, F.S. Donaires, M.C. Picinato, R.C. Giorgenon, B.A. Santana, R.N. Pimentel, D.L. Keefe, R.T. Calado, R.A. Ferriani, et al., Telomere length and telomerase activity in immature oocytes and cumulus cells of women with polycystic ovary syndrome, Reprod. Sci. 27 (6) (2020) 1293–1303.

[17] M.Z. Levy, R.C. Allsopp, A.B. Futcher, C.W. Greider, C.B. Harley, Telomere end-replication problem and cell aging, J. Mol. Biol. 225 (4) (1992) 951–960.

[18] O. Arino, M. Kimmel, G.F. Webb, Mathematical modeling of the loss of telomere sequences, J. Theoret. Biol. 177 (1) (1995) 45–57.

[19] J. op den Buijs, P.P. van den Bosch, M.W. Musters, N.A. van Riel, Mathematical modeling confirms the length-dependency of telomere shortening, Mech. Ageing Dev. 125 (6) (2004) 437–444.

[20] R. Portugal, M. Land, B.F. Svaiter, A computational model for telomere-dependent cell-replicative aging, Biosystems 91 (1) (2008) 262–267.

[21] J.A. Wattis, Q. Qi, H.M. Byrne, Mathematical modelling of telomere length dynamics, J. Math. Biol. 80 (4) (2020) 1039–1076.

[22] A. Portillo, E. Varela, J. García-Velasco, Mathematical model to study the aging of the human follicle according to the telomerase activity, J. Theoret. Biol. 462 (2019) 446–454.

[23] N.L. Wesch, L.J. Burlock, R.J. Gooding, Critical telomerase activity for uncontrolled cell growth, Phys. Biol. 13 (4) (2016) 046005.

[24] A. Portillo, C. Peláez, Mathematical modelling of ageing acceleration of the human follicle due to oxidative stress and other factors, Math. Med. Biol.: J. IMA 38 (3) (2021) 273–291.

[25] T. Von Zglinicki, Oxidative stress shortens telomeres, Trends Biochem. Sci. 27 (7) (2002) 339–344.

[26] M.H. Protter, H.F. Weinberger, Maximum Principles in Differential Equations, Springer Science & Business Media, 2012.

[27] A. Friedman, Partial Differential Equations of Parabolic Type, Courier Dover Publications, 2008.

[28] W.J. Golz, J.R. Dorroh, The convection-diffusion equation for a finite domain with time varying boundaries, Appl. Math. Lett. 14 (8) (2001) 983–988.

[29] W. Wang, H. Chen, R. Li, N. Ouyang, J. Chen, L. Huang, M. Mai, N. Zhang, Q. Zhang, D. Yang, Telomerase activity is more significant for predicting the outcome of IVF treatment than telomere length in granulosa cells, Reproduction 147 (5) (2014) 649–657.

[30] A. Gougeon, Regulation of ovarian follicular development in primates: facts and hypotheses, Endocr. Rev. 17 (2) (1996) 121–155.

[31] C.L. Wagner, V.S. Hanumanthu, C.C. Talbot, R.S. Abraham, D. Hamm, D.L. Gable, C.G. Kanakry, C.D. Applegate, J. Siliciano, J.B. Jackson, et al., Short telomere syndromes cause a primary T cell immunodeficiency, J. Clin. Invest. 128 (12) (2018) 5222–5234.

[32] X. Xu, X. Chen, X. Zhang, Y. Liu, Z. Wang, P. Wang, Y. Du, Y. Qin, Z.-J. Chen, Impaired telomere length and telomerase activity in peripheral blood leukocytes and granulosa cells in patients with biochemical primary ovarian insufficiency, Hum. Reprod. 32 (1) (2017) 201–207.

[33] S. Butts, H. Riethman, S. Ratcliffe, A. Shaunik, C. Coutifaris, K. Barnhart, Correlation of telomere length and telomerase activity with occult ovarian insufficiency, J. Clin. Endocrinol. Metab. 94 (12) (2009) 4835–4843.

[34] V. Gaysinskaya, S.E. Stanley, S. Adam, M. Armanios, Synonymous mutation in DKC1 causes telomerase RNA insufficiency manifesting as familial pulmonary fibrosis, Chest 158 (6) (2020) 2449–2457.

[35] L.G. Robinson, R. Pimentel, F. Wang, Y.G. Kramer, D.C. Gonullu, S. Agarwal, P.A. Navarro, D. McCulloh, D.L. Keefe, Impaired reproductive function and fertility preservation in a woman with a dyskeratosis congenita, J. Assist. Reprod. Genet. 37 (5) (2020) 1221–1225.

[36] N.R. Treff, J. Su, D. Taylor, R.T. Scott Jr., Telomere DNA deficiency is associated with development of human embryonic aneuploidy, PLoS Genet. 7 (6) (2011) e1002161.